Published online 29 March 2011 *Nucleic Acids Research, 2011, Vol. 39, No. 13* ***5439–5448***
doi:10.1093/nar/gkr175

Monitoring the reversible B to A-like transition of DNA in eukaryotic cells using Fourier transform infrared spectroscopy

Donna R. Whelan[1], Keith R. Bambery[1], Philip Heraud[1,2], Mark J. Tobin[3], Max Diem[4], Don McNaughton[1] and Bayden R. Wood[1,*]

[1]Center for Biospectroscopy and School of Chemistry, [2]Monash Immunology and Stem Cell Laboratories, Monash University, Clayton, Victoria, 3800 [3]Australian Synchrotron, 800 Blackburn Road, Clayton, Victoria 3168, Australia and [4]Department of Chemistry and Chemical Biology, Northeastern University, Boston, MA 02115, USA

Received December 20, 2010; Revised and Accepted March 10, 2011

ABSTRACT

The ability to detect DNA conformation in eukaryotic cells is of paramount importance in understanding how some cells retain functionality in response to environmental stress. It is anticipated that the B to A transition might play a role in resistance to DNA damage such as heat, desiccation and toxic damage. To this end, conformational detail about the molecular structure of DNA has been derived primarily from *in vitro* experiments on extracted or synthetic DNA. Here, we report that a B- to A-like DNA conformational change can occur in the nuclei of intact cells in response to dehydration. This transition is reversible upon rehydration in air-dried cells. By systematically monitoring the dehydration and rehydration of single and double-stranded DNA, RNA, extracted nuclei and three types of eukaryotic cells including chicken erythrocytes, mammalian lymphocytes and cancerous rodent fibroblasts using Fourier transform infrared (FTIR) spectroscopy, we unequivocally assign the important DNA conformation marker bands within these cells. We also demonstrate that by applying FTIR spectroscopy to hydrated samples, the DNA bands become sharper and more intense. This is anticipated to provide a methodology enabling differentiation of cancerous from non-cancerous cells based on the increased DNA content inherent to dysplastic and neoplastic tissue.

INTRODUCTION

In the last two decades the structure, rather than the genetic code, of DNA has become a focus area for research into cancer cause and treatment, genetic diseases and gene regulation (1). Of increasing interest is the transition of B- to A-DNA and the envisaged important role that A-DNA plays in cells. A-DNA or A-like DNA [where the DNA conformation has predominately A-like DNA parameters (2,3)] is considered to be the induced conformation predominant in many DNA–protein interactions including several polymerase reactions (4,5), sequence specific protein–DNA recognition via hydrophobic interactions (6), and in many other interactions with a myriad of biologically important ligands (7) and counter-ions (8). Furthermore, RNA/DNA helices, such as those necessary for transcription, are predicted to exist in an A-like helix because of the inability of RNA/DNA helices to exist in a B-like form due to van der Waals crowding of the ribose C2′-oxygen of the RNA (9,10). Of particular interest, A-DNA has been hypothesized as a defense mechanism against DNA damage in the spores of Gram-positive bacteria (11). This is in accordance with the known ability of A-DNA to resist UV radiation-induced damage (12) and radiosensitization by external agents (13). It is anticipated that the B to A transition might play a role in resistance to other forms of DNA damage such as heat, desiccation and toxic damage (11). This research has so far been confined to *in vitro* DNA and a small selection of spores where the presence of small acid soluble proteins (SASPs) has been demonstrated as inducing a B- to A-like conformational change in response to stress (11,12). It is hypothesized that

*To whom correspondence should be addressed. Tel: +61 3 9905 5721; Fax: +61 3 9905 4597; Email: bayden.wood@monash.edu

The authors wish it to be known that, in their opinion, the first and last authors should be regarded as joint First Authors.

the main role of the SASPs is to induce the conformational transition and that the A-like DNA then plays a major role in the resistance to DNA damage (11). This is the only known instance of an overall B to A transition suggested to occur *in situ* (i.e. where the DNA exists in its native state and is inside the cell) and it has only been demonstrated through *in vitro* and crystallographic experiments (11,12). Hitherto, the majority of the research into DNA conformation has been restricted to methods that are either purely *in vitro* or dependent on preparative techniques which compromise the integrity of the cell. The best evidence for a B-like structure of DNA *in situ* consequently comes from crystallographic experiments on intact crystallized nucleosomes (14) with supporting evidence supplied by *in vitro* Fourier transform infrared (FTIR) spectroscopic demonstration of the overall B-philic preference of native DNA in synthesized cellular conditions (15).

Here we present, for the first time, the detection of DNA conformational detail *in situ* using FTIR spectroscopy on hydrated eukaryotic cells. B-like DNA is detected in live cells and an overall shift to A-like DNA upon dehydration is observed. Subsequent rehydration of these cells reveals that the DNA returns to the native B-like form detected in the live cells. The exact mechanism and the implications of this overall genomic B to A to B transition remain uncertain; however, the ability of *in situ* DNA to maintain its structure via a transition to A-DNA when dehydrated enabling a complete return to the native B-like state upon rehydration indicates some ability to regain functionality under similar circumstances. This is unsurprising, though important evidence, when considered in relation to the family of spores known to employ an overall shift to an A-like conformation as a defense mechanism (11,12) and on the local scale in all eukaryotic cells where short temporary stretches of A-like DNA are no longer considered infrequent (4–8). Here, however, we show that dehydration of eukaryotic cells with no documented A-like DNA-based defense mechanism does induce a consistent B to A transition and that this transition appears to enable a return to the native B-like DNA structure upon rehydration.

Furthermore, the application of FTIR spectroscopy to hydrated cells that allowed the detection of conformational detail demonstrates the importance of the cell hydration state in DNA band elucidation. In the past, most infrared spectroscopy of biological samples has been conducted on dehydrated cells and tissue because of the strong overlap of the water deformation mode in the amide region (1710–1500 cm^{-1}) (16). Here, we demonstrate that in the dehydrated state some DNA marker bands are more difficult to detect and interpret because of band broadening and intensity loss whereas in the hydrated state, these bands are more easily observed. This result has far-reaching implications for cancer diagnosis using FTIR spectroscopy (17) where the detection of the relative DNA concentration is an important marker for dysplasia (16) and neoplasia (18).

MATERIALS AND METHODS

FTIR spectroscopic techniques

To demonstrate the reproducibility of this research, three different FTIR spectroscopic techniques were used. Transmission FTIR (T-FTIR) was used primarily to record the spectral series of the reference samples of double- and single-stranded DNA and RNA. This technique requires the compression of a very thin smear of liquid between infrared-transparent plates and the transmission of the infrared beam through the sample. Synchrotron-FTIR (S-FTIR), while operating in an identical manner, allows for a high photon flux infrared beam and diffraction limited resolution allowing the targeting of individual cells. Attenuated Total Reflectance FTIR (ATR-FTIR) takes advantage of the evanescent wave effect that occurs when light undergoes total internal reflectance inside a crystal. By positioning a sample flush against the sampling crystal, the infrared beam penetrates a few micrometers and the resultant spectrum corrected to provide essentially an absorption spectrum. ATR-FTIR spectra were acquired of all samples and potential artifacts from limited penetration of the infrared beam were ruled out by comparison with spectra taking using T-FTIR and S-FTIR.

FTIR spectra of double- and single-stranded DNA and RNA

Wet films were prepared using single-stranded DNA from salmon testes (≥65% single stranded, mol. wt. ~50 kb) and double-stranded DNA from calf thymus (mol. wt. 8–15 kb; 42% GC content) (Sigma, St Louis, MO, USA) by dissolving ~1 mg/ml in ultrapure water at 4°C. RNA from the yeast *Saccharomyces cerevisiae* was similarly prepared (2 mg/ml, Sigma). Application of ~50 µl of sample solution between two calcium fluoride windows was found to give good signal. Spectra were collected every 30 s in ambient conditions until no difference was recorded between spectra taken over an hour. Rehydration was achieved by placement of ~500 µl wet sample on a single calcium fluoride window and drying under nitrogen. Ultrapure water was then introduced onto the calcium fluoride window directly beside the beam path. Spectra were taken every 20 s and water was added to the same spot to keep a reserve of ~50 µl. In all benchtop experiments, 64 co-added scans were taken over the region 4000–800 cm^{-1} with a resolution of 6 cm^{-1}. All transmission spectra were obtained using a Bruker IFS Equinox FTIR system. For ATR-FTIR measurements the same system was paired with a Golden Gate single bounce diamond micro-ATR spectrometer. Second derivatives with a Savitzky-Golay smoothing point value of nine and peak picking were performed with OPUS software, version 6.0.

FTIR of chicken erythrocytes

Chicken erythrocytes were purchased in lithium heparin and used within 2 weeks of bleeding (AIV&MS, Adelaide, Australia). All samples were washed as previously detailed (19). Erythrocytes were suspended 1 ml/ml in isotonic

saline and ~20 μl of the suspension was applied to a single pass diamond window ATR. For S-FTIR measurements, 40 μl of cell suspension was smeared on a calcium fluoride window and a 50-μl droplet of isotonic saline placed at the periphery of the window to keep the sample hydrated during calibration. Single blood cells were identified within 50 μm of the droplet and spectra were collected continuously by co-adding 128 scans at resolution 6 cm^{-1} until dehydrated using a Bruker Vertex V80v spectrometer coupled with a Hyperion 2000 microscope with a liquid nitrogen cooled narrow-band mercury cadmium telluride (MCT) detector at the Australian Synchrotron microspectroscopy infrared beamline (20). Rehydration experiments were performed using a purpose built dual window transmission device. Chicken erythrocytes are placed on one window of this device and rapidly desiccated under vacuum. The device is then reassembled and water gradually introduced using a syringe. The water pools in a cavity just below the windows enabling the water vapor to gradually rehydrate the cells. Spectra were recorded in transmission mode on a Bruker IFS28/B equipped with a deuterated triglycine sulfate (DTGS) detector at 6 cm^{-1} with 32 scans co-added. Nuclei were extracted from erythrocytes using Triton X-100 as has been detailed previously (21). Nuclei were then suspended in isotonic saline 1 ml/ml and measurements taken in the same manner as outlined for intact erythrocyte experiments.

FTIR of fibroblasts L-929 and lymphocytes

Mouse cancerous fibroblasts clone line 929 were cultured in media as has been outlined previously (22). They were taken from culture at passage 15–25 by trypsinizing and suspended in isotonic saline 0.25 mg/ml. Immediately after suspension, they were transferred to the ATR diamond window where dehydration was achieved under nitrogen. Rehydration required the slow introduction of water to the dry film and was achieved by careful clamping of the film between the diamond window and sapphire pressure crystal. Isotonic saline was introduced by pipette (10 μl) to the exposed diamond window and allowed to seep into the fibroblast film. Spectra were collected as above but with no extended time interval between measurements. Synchrotron measurements of single fibroblasts were achieved using the same procedure used for the erythrocytes. Mammalian lymphocytes were separated from whole blood as previously described (23). FTIR spectroscopic measurements were recorded of rehydrating lymphocytes using the purpose built dual window transmission device and the same methodology and instrumental parameters that were adopted for the rehydrated erythrocytes.

Principal components analysis

The bilinear modeling technique principal component analysis (PCA) was performed using 'The Unscrambler' software suite, version 9.2 (CAMO, Norway). This method, designed to reduce the dimensionality of the data set, decomposes the spectral series into principal components (PCs). Each PC is orthogonal to the previous PC with the variance described by each subsequent PC decreasing. Scores plots, which plot one PC against another, enable visualization of the position of each spectrum in 1-, 2- or 3-dimensional space relative to the other spectra. The loadings plot of a particular PC depicts the variables (wavenumber) responsible for the distribution of the spectra on the scores plot of that PC. The magnitude of a particular variable on the loadings plot corresponds to the degree to which it contributed to the variance in the scores plot.

For PCA, second derivative spectra were converted from an OPUS format to JCAMP files and imported directly to The Unscrambler software suite. PCA was performed on the 1800–800 cm^{-1} region and no samples were excluded based on outlier determination. PC1 versus PC2 scores plots and PC1 loadings plots were plotted for erythrocytes, fibroblasts, nuclei and DNA in response to hydration.

RESULTS

FTIR spectra of double- and single-stranded DNA and single-stranded RNA

The FTIR spectrum of A- and B-DNA has been studied exhaustively in the past (24–27) with multiple bands assigned and identified as indicative of specific conformations. Nonetheless, to ensure no artifacts due to procedural differences between previous work and our research, reference series of DNA and RNA were acquired according to the experimental procedures used for acquisition of cell spectra. Both the dehydration and rehydration series of double-stranded DNA are in excellent accordance with previous work and show the distinct spectral signatures of B- and A-DNA (24–29). Moreover, the infrared marker bands for A- and B-DNA focused on in this work have been used frequently in the past to differentiate between DNA conformations involved in drug and protein interactions with DNA and correlated to other techniques used to determine DNA conformation such as circular dichroism (30–32), X-ray crystallography (33) and UV-Vis spectroscopy (31,32).

The first and last spectrum of a gradual dehydration series of chicken erythrocytes and isolated double-stranded DNA (dsDNA) are shown in Figure 1A and B with the main DNA conformational bands highlighted and assigned in Table 1. These spectra are indicative of fully hydrated cells and DNA and cells and DNA dehydrated to equilibrium with the atmosphere. Second derivatives of the spectra in Figure 1A and B are shown in Figure 1C and D. The full underivatized and second derivative spectra series of DNA dehydration and a rehydration are presented in the Supplementary Figures S1 and S2 along with underivatized and second derivative erythrocyte series (Supplementary Figure S3). Second derivatives enable easier differentiation between overlapping bands and are used for identifying peak positions unless otherwise noted. Detailed assignments for all cells and biomolecules analyzed are presented in Supplementary Table S1. Small differences in initial and final band positions are the result of hysteresis of the phase transitions. All measurements were performed in triplicate

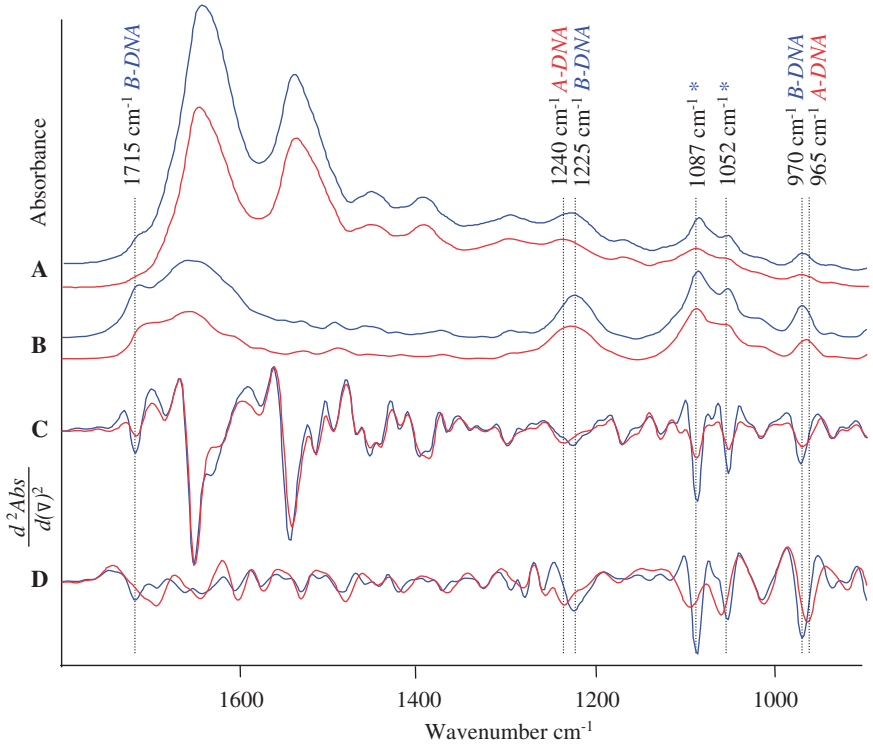

Figure 1. Fully hydrated (blue) and dehydrated (red) spectra of (**A**) intact chicken erythrocytes and (**B**) double-stranded DNA and the corresponding second derivatives for (**C**) intact chicken erythrocytes and (**D**) double-stranded DNA. Important DNA conformation bands are indicated and approximate band position given. Asterisk denotes bands which lose significant intensity upon B–A transition.

Table 1. Important DNA conformational band assignments and approximate peak positions for B- and A-DNA

Assignment	B-DNA (cm^{-1})	A-DNA (cm^{-1})
Base pair carbonyl ν(C═O)	1717	1712
C2′/C3′-endo deoxyribose	1422	1418
Antisymmetric phosphate $\nu_{sym}(PO_2^-)$	1225	1238
C3′endo-sugar phosphate	Absent	1185
Symmetric phosphate ν (PO_2^-)	1087	1087*
Backbone ν(C–O)	1051	1051*
Backbone ν(C–C)	970	965

*Indicates a significant loss of intensity.

with calculated standard deviations quoted alongside average band positions and rounded off to the nearest whole number. Fully hydrated DNA exists in the B-conformation and accordingly the phosphate antisymmetric stretching vibration, $\nu_{asym}(PO_2^-)$, is located at 1225 ($\pm 2\,cm^{-1}$). Other markers for B-DNA include a peak at 1422 ($\pm 1\,cm^{-1}$) assigned to the C2′-endo deoxyribose vibration (27) and a peak at 936 ($\pm 1\,cm^{-1}$) previously assigned to a paired AT base vibration (27). Other prominent DNA infrared absorption bands include the phosphate symmetric stretching vibration, $\nu_{sym}(PO_2^-)$, ($1087 \pm 1\,cm^{-1}$) which appears sharp and more intense than the C–O stretch of the backbone, ν(C–O), ($1051 \pm 1\,cm^{-1}$) and the peak at 969 ($\pm 1\,cm^{-1}$) assigned to the C–C stretch of the DNA backbone, ν(C–C). Each of these peaks undergoes a shift or change in intensity as a consequence of conformational change from B-DNA to A-DNA or from A-DNA to B-DNA in double-stranded films. One of the main markers for the B to A transition is the shift of the $\nu_{asym}(PO_2^-)$ from $1225\,cm^{-1}$ ($\pm 2\,cm^{-1}$) to 1238 ($\pm 1\,cm^{-1}$) during dehydration. Upon rehydration this band shift reverses. In the underivatized series an underlying peak at 1211 ($\pm 1\,cm^{-1}$) attributed to a thymine vibration (34) overlaps the $\nu_{sym}(PO_2^-)$ and obscures this shift. The sugar vibration shifts to 1420 ($\pm 1\,cm^{-1}$) in accordance with the change from C2′-endo to C3′-endo. The band at $936\,cm^{-1}$ ($\pm 1\,cm^{-1}$) lacks intensity in the A-form and hence is a B-DNA marker. Similarly, the backbone $\nu_{sym}(PO_2^-)$ and ν(C–O) stretch vibrations at 1088 ($\pm 1\,cm^{-1}$) and 1051 ($\pm 1\,cm^{-1}$), respectively, both lose intensity and shape upon dehydrating. A strong shoulder is observed around $1100\,cm^{-1}$ and a shoulder peak at 1067 ($\pm 1\,cm^{-1}$) is identified in the A-DNA second derivative spectra. Finally, the ν(C–C) stretch red shifts to $966\,cm^{-1}$ ($\pm 1\,cm^{-1}$) in A-DNA.

Interestingly, examination of the underivatized and second derivative dehydration series of single-stranded DNA (Supplementary Figures S1A and S2A) also show each of these suggested B- and A-DNA marker bands including the $\nu_{asym}(PO_2^-)$ [1224 ($\pm 2\,cm^{-1}$)–1235 ($\pm 2\,cm^{-1}$)], the C2′/C3′-endo deoxyribose [1422 ($\pm 1\,cm^{-1}$)–1417 ($\pm 1\,cm^{-1}$)] and a band previously attributed to the AT base pair vibration [936 ($\pm 1\,cm^{-1}$)]. The shifts and loss of intensity in the backbone vibrations in the spectral series of

single-stranded DNA are also very similar to those seen in double-stranded DNA. Only two points of difference are discernible in the second derivative. A shoulder peak at 1184 ($\pm 1\,cm^{-1}$) considered to be a sugar phosphate vibration with a high contribution from C3′-endo type puckering is seen most strongly in the dehydrated double-stranded DNA spectra of both the dehydration and rehydration series but not in the single-stranded spectra (27). Furthermore, the most striking contrast between the spectral series of single and double-stranded DNA is the presence of a strong shoulder peak at 1715 ($\pm 2\,cm^{-1}$) in the double-stranded form only and attributed to a carbonyl stretching vibration (23). In contrast, the single-stranded DNA spectra show a strong peak at 1693 ($\pm 1\,cm^{-1}$) and no obvious shoulder at $1715\,cm^{-1}$. The second derivative spectra highlight a peak at 1717 ($\pm 1\,cm^{-1}$) in only the most hydrated spectra but this is not nearly as intense as the peak in the spectra of the double-stranded DNA and is explained by the unavoidable incidence of random duplexing in single-stranded DNA while in solution. Based on this evidence and previous research, the absorption peaks in the 1720–1710 cm^{-1} region are attributed to nucleic bases with strong base stacking and pairing interactions while the red shifted absorption at $\sim 1690\,cm^{-1}$ can be attributed to bases with weaker interactions (23). This base pair vibration at 1720–1710 cm^{-1} is thus considered diagnostic of duplexed DNA and when the remaining infrared absorptions are seen in conjunction, they can be regarded as diagnostic of B- and A-form DNA. The ability to undergo multiple dehydration/rehydration cycles with the base pairing vibration and $1184\,cm^{-1}$ backbone vibration consistently apparent in the spectra provides strong evidence that the duplexed DNA has not denatured or transformed to single-stranded DNA during dehydration and is truly returning to pure B-DNA form.

Spectral series for the dehydration and rehydration of RNA were also acquired with the rehydration series and second derivative series shown (Supplementary Figures S1B and S2B, respectively). The $\nu_{asym}(PO_2^-)$ was observed at 1242 ($\pm 1\,cm^{-1}$) overlapping a RNA ribose specific band at 1215 ($\pm 4\,cm^{-1}$) (27) regardless of the state of hydration. The $\nu_{sym}(PO_2^-)$, ν(C–O) and ν(C–C) are consistent in position with those observed in the dehydrated DNA [1083 ($\pm 3\,cm^{-1}$), 1057 ($\pm 2\,cm^{-1}$) and 965 ($\pm 4\,cm^{-1}$), respectively] though somewhat diminished. The nucleic base carbonyl vibration in RNA was detected at 1690 ($\pm 1\,cm^{-1}$) similar to the single-stranded series. Again, only a small peak at 1712 ($\pm 1\,cm^{-1}$) was observed and is again attributable to random duplexing. Most importantly, the added hydroxyl group at the 2′-position of ribose rings in RNA introduces sharp RNA-specific infrared absorptions at 1125 ($\pm 7\,cm^{-1}$) and 993 ($\pm 1\,cm^{-1}$). These particular peaks are considered diagnostic of the contribution of RNA in the nucleic acid backbone vibrations observed in cell spectra (27).

FTIR spectra of chicken erythrocytes

The first and last second derivative spectrum from a dehydration and rehydration series performed on extracted chicken erythrocyte nuclei are shown in Figure 2A and B, respectively. The full series is depicted in Supplementary Figure 4. Chicken erythrocytes were used for these experiments because of the large nucleus and relatively high DNA concentration, furthermore, because the nucleus is almost completely metabolically and transcriptionally inactive, the contents of the cells are conserved between samples and the interference from other cell components is confined to well-characterized macromolecules. As such the major peaks in the raw spectra are those attributed either to nucleic acid or protein. All the nucleic acid peaks documented in the hydrated double-stranded DNA as indicative of B-DNA are present in the hydrated nuclei spectra and are observed to be predominantly due to duplexed DNA as supported by the presence

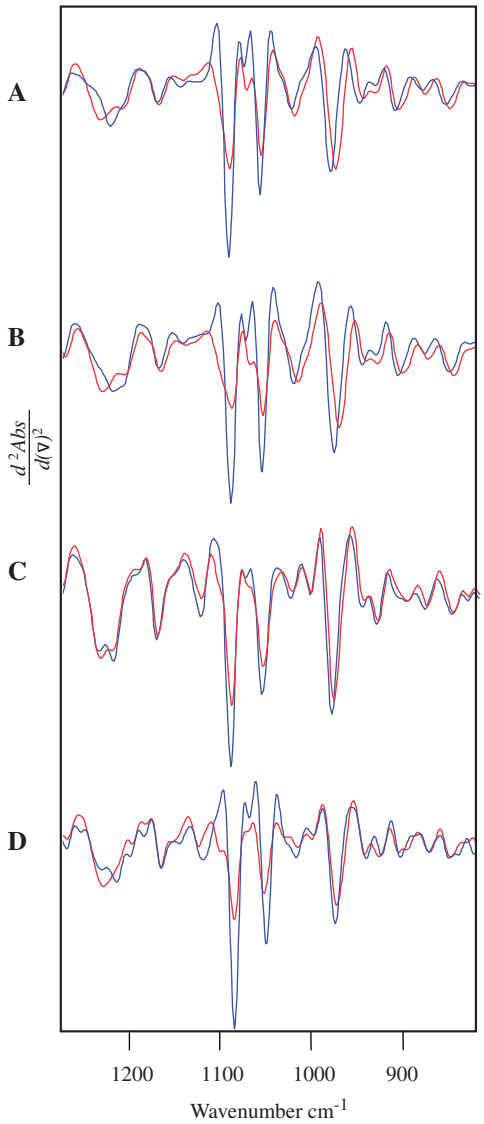

Figure 2. Second derivative spectra of fully hydrated (blue) and dehydrated (red) (**A**) extracted chicken erythrocyte nuclei undergoing dehydration (ATR-FTIR), (**B**) extracted chicken erythrocyte nuclei undergoing rehydration (ATR-FTIR), (**C**) mammalian cancerous fibroblasts (L-929) undergoing rehydration (ATR-FTIR) and (**D**) mammalian lymphocytes undergoing rehydration (T-FTIR).

of the strong base pairing vibration at ~1717 cm^{-1} and the lack of RNA marker bands. Moreover, the shifts and changes in band profile identified in the DNA spectral series as indicative of the B to A transition are observed upon dehydration of the erythrocyte nuclei. The fully hydrated second derivative spectrum from the end of a rehydration series shown in Figure 2B (blue spectrum) demonstrates no detectable difference with the initial hydrated nuclei spectrum (Figure 2A, blue spectrum) and is in concordance with the A to B transition seen in rehydrating DNA films. This demonstrates that the DNA remains not only intact and duplexed but also returns to the initial native structure.

The ATR-FTIR dehydration series on intact chicken erythrocytes depicted in Figure 1A was duplicated with S-FTIR measurements of single cells dehydrating and T-FTIR measurements of bulk erythrocytes rehydrating (Supplementary Figure 5). Results across all methods were concordant with rehydration resulting in identical spectra to those taken of intact hydrated native erythrocytes. Peak position and intensity in the backbone region of the spectra (1300–800 cm^{-1}) remain the same as those demonstrated and attributed to double-stranded DNA in extracted nuclei and in the native DNA films. The peak shifting and intensity changes are also in excellent agreement with B-like DNA in the hydrated cell spectra and A-like DNA in the dehydrated cell spectra.

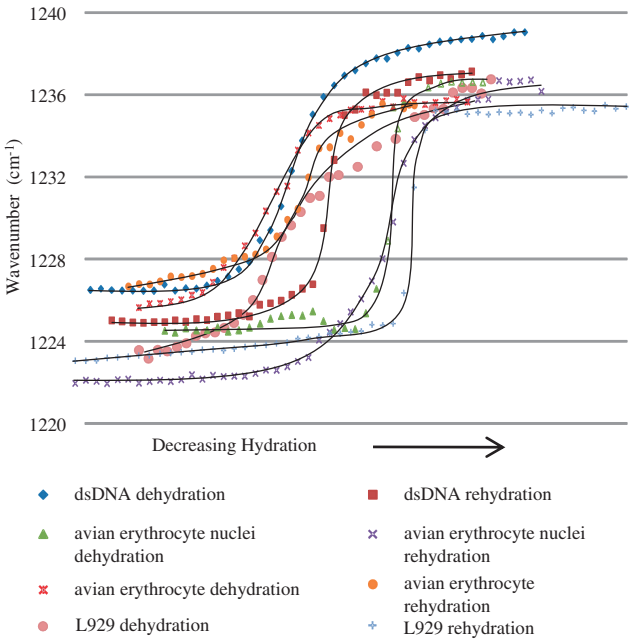

Figure 3. Trend plot showing the shift of peak position of the antisymmetric phosphate stretching vibration from ~1224 to 1236 cm^{-1} with decreasing/increasing hydration. Series plotted for dehydration and rehydration are indicative of trends seen across all experiment types.

FTIR spectra of fibroblasts and lymphocytes

The full underivatized and second derivative ATR-FTIR spectral series for the rehydration of a population of cancerous mouse fibroblasts (cell line L-929) are presented in Supplementary Figure 6. A similar T-FTIR series for lymphocytes is presented in Supplementary Figure 7. The results from the fibroblast ATR experiments were also duplicated on a single cell using S-FTIR and depicted in Supplementary Figure 8. Figure 2C shows the first and last spectrum of an ATR-FTIR series of rehydrating fibroblasts while Figure 2D show the first and last spectrum for a T-FTIR series of rehydrating lymphocytes. In these series the higher phospholipid and collagen content of a functional fibroblast is expected to contribute to the spectra and complicate the interpretation of the region $<1300\,cm^{-1}$. Despite these anticipated difficulties, the presence of the DNA base pair vibration is observed at ~1717 cm^{-1} in both the fibroblast and lymphocyte series. The neighboring absorption at ~1735 cm^{-1} is attributed to the phospholipid ester carbonyl and is distinctly separated from the base pair vibration in the second derivatives. Remarkably, both fibroblast and lymphocyte series are observed to have the marker bands associated with the B to A transition upon dehydration and the A to B transition upon rehydration. However, it should be noted that instead of a clear red shift of the $\nu_{asym}(PO_2^-)$ upon rehydration in the fibroblast and lymphocyte series there appear to be two overlapping bands in all of the spectra with a gradual transition from a more intense 1237 cm^{-1} in the fully dehydrated spectra to a more intense 1222 cm^{-1} in the fully rehydrated. This is reproduced in the dehydration spectra of the single fibroblast cell and is due to the presence of non-DNA phosphates such as phospholipids, RNA and phosphorylated proteins in the fibroblasts. Nonetheless, the changing intensity provides evidence for the DNA phosphate absorption changing with the conformational transition.

Spectral trend analysis

To evaluate the similarity of the changes indicative of a B to A/A to B transition and the changes observed in nuclei and cell spectra the spectral features in two marker band regions have been plotted. Because of the nature of the experiments a precise hydration value cannot be calculated and consequently there is no numerical value on the *x*-axis. In Figure 3 the peak position of the $\nu_{asym}(PO_2^-)$ is shown in relation to the hydration level of the sample. All nuclei and cell samples, regardless of whether the experiment was a rehydration or dehydration and the type of FTIR used, show the same characteristic sigmoidal-shape trend as the B to A transition of double-stranded DNA. Furthermore, all trend curves display similar start and end points indicating the $\nu_{asym}(PO_2^-)$ peak to have similar positions for all samples in the fully hydrated and dehydrated states. This further supports the hypothesis that the DNA within the cells is returning to the native B-like state upon rehydration. Figure 4 shows the trend plot of the peak position of the ν(C–C) with relation to the level of sample hydration. Again, all nuclei and cell types under all experimental conditions show a very similar trend to that observed during the B–A and A–B transition of double-stranded DNA. Unlike the sigmoidal profile of the transition of the $\nu_{asym}(PO_2^-)$ peak shown in Figure 3, this transition is

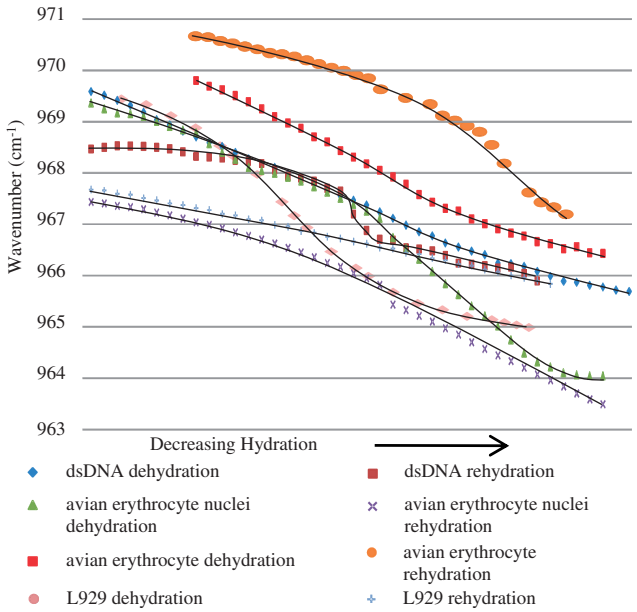

Figure 4. Trend plot showing the shift of peak position of the C–C stretching vibration from ~969 to ~965 cm^{-1} with decreasing/increasing hydration. Series plotted for dehydration and rehydration are indicative of trends seen across all experiment types.

gradual, approximating a linear relationship over the duration of the experiment.

Principal component analysis

Further evidence of the B to A transition in cell samples was assessed using the multivariate statistical method of PCA. This analysis was performed on the second derivative data of each series to examine the spread and the cause of the major variance in the spread of each spectral series. The resulting scores plots show the relative position of each spectrum in a series in the 2D space formed by the first and second principal components (PC1 and PC2) of the analysis. PCA performed on second derivative series of double-stranded DNA dehydration, chicken erythrocyte nuclei rehydration, chicken erythrocyte dehydration and fibroblast rehydration resulted in very similar separation of the spectra in each series into a parabolic scatter plot along PC1 and PC2 with the most hydrated spectra having the most negative PC1 scores and the most dehydrated spectra having the most positive PC1 Scores, regardless of the nature of the experiment. Separation along PC1 was sequential for all series.

The explained variance for PC1 across the second derivative spectral region 1800 to 800 cm^{-1} is 93% for both double-stranded DNA and chicken erythrocyte nuclei and 96% for both chicken erythrocytes and fibroblasts. The variance associated with PC2 is 3–5% and examination did not yield any significant pattern. Figure 5 shows the loadings associated with PC1 of each of the four samples analyzed. Peaks in the loadings plot correlate to the negative scores (the more hydrated spectra) while troughs correlate to the positive scores (the more dehydrated spectra). The magnitude of a peak or trough is indicative of the degree to which that particular infrared absorption influenced the spread of the scores plot: the largest peaks/troughs caused the most variance. Examination of the loadings plots demonstrated that interference from the water deformation mode did not affect the PCA to any significant degree. Instead, the most significant causes for variance are largely confined to DNA-related absorbances. All four loadings demonstrate the prominence and consistence of the known B to A-DNA marker bands, including those used to construct the trend plots (Figures 3 and 4). The characteristic $\nu_{asym}(PO_2^-)$ shift is evident with peaks at 1223 (± 2 cm^{-1}) and troughs at 1240 (± 5 cm^{-1}). The shift of the ν(C–C) of the backbone seen in the underivatized spectra series and plotted in Figure 4 is further amplified by PCA with a peak at 973 (± 2 cm^{-1}) attributed to the hydrated spectra and a trough at 958 (± 2 cm^{-1}) attributed to the dehydrated spectra. The $\nu_{sym}(PO_2^-)$ band was observed to lose intensity and broaden upon dehydration and, accordingly, the PC1 loading identifies $\nu_{sym}(PO_2^-)$ as contributing strongly to hydrated spectra (1087 $\pm$ 1 cm^{-1}) while a trough at 1099 $\pm$ 1 cm^{-1} is associated with the dehydrated spectra. This is in good agreement with the second derivative spectra that similarly show a shoulder at 1100 cm^{-1} for dehydrated spectra. The remaining loadings from 1100 to 800 cm^{-1} are remarkably similar because protein absorptions do not interfere in this region as strongly

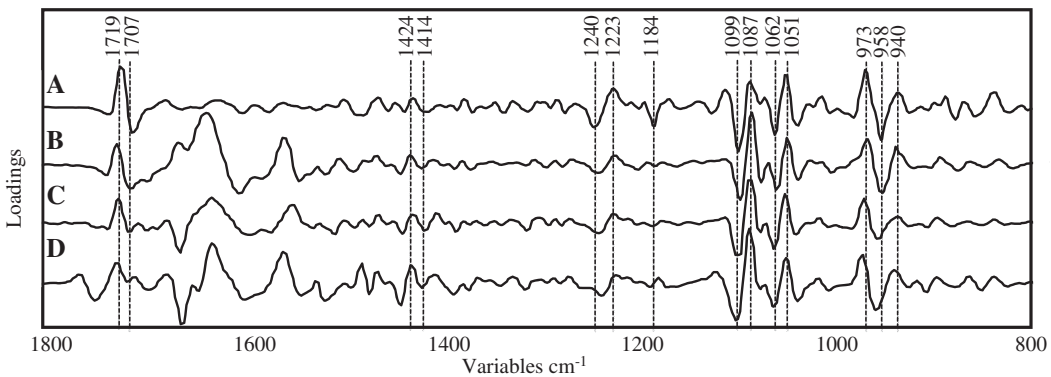

Figure 5. Principal component 1 loadings plots for (**A**) dehydrating double-stranded DNA, (**B**) rehydrating chicken erythrocyte nuclei, (**C**) dehydrating chicken erythrocytes and (**D**) rehydrating mammalian fibroblasts. In all cases, peaks are attributed as causing variance in hydrated sample spectra while troughs are attributed as causing variance in dehydrated sample spectra.

as they do in the typical Amide I, II and III regions. The shoulder at 1062 ($\pm 1\,cm^{-1}$) is attributed to the dehydrated spectra while the sharp ν(C–O) ($1051 \pm 1\,cm^{-1}$) contributes most to the hydrated spectra. Furthermore, the smaller peaks and troughs seen in the 1100–800 cm^{-1} region are largely concordant and demonstrate potential as further diagnostic bands for the presence of B- and A-like DNA.

Other diagnostic bands include the A-DNA marker band at 1184 ($\pm 1\,cm^{-1}$). While it is quite intense as a trough in the PC1 loading of native DNA it is a somewhat smaller trough in the three other PC1 loadings demonstrating the presence of only a proportion of pure A-DNA because it is not as strong as would be predicted from the spectrum of pure A-DNA. The PC1 loadings also display a peak at 1719 ($\pm 1\,cm^{-1}$) and a trough at 1707 ($\pm 2\,cm^{-1}$) consistent with the presence of the base pair carbonyl vibration and the red shift of this vibration during a B to A type transition.

DISCUSSION

We demonstrate, using FTIR spectroscopy, the detection of an overall conformational B-like to A-like transition in the DNA of several eukaryotic cells and the reverse A-like to B-like transition upon rehydration. Furthermore, we show that spectra of hydrated cells, including cells previously considered to yield little or no absorptions from DNA, produce sharp DNA-specific peaks in the hydrated state which broaden and lose intensity when dehydrated.

Intense DNA peaks detectable in all samples in the backbone region (1300–800 cm^{-1}) were assigned according to previous work conducted on DNA conformation using FTIR spectroscopy (24–29). Peaks assigned to the vibrational modes of the nucleic bases are more difficult to observe due to their smaller intensities compared to the backbone vibrations especially in the 1700–1300 cm^{-1} region where overlapping protein bands dominate. The base pairing vibration at 1717 cm^{-1} is easily discernible in the second derivative spectra and PC1 loadings plot of each cell series investigated and is a definitive marker for duplexed nucleic acids because it is only in this state that the base stacking and hydrogen bond effects can combine to shift the nucleic acid carbonyl vibration from 1690 cm^{-1} (as observed in single-stranded DNA and RNA) to 1717 cm^{-1}. A confounding contribution from RNA in the cell spectra is discounted due to the lack of or, in the case of the fibroblasts and lymphocytes, comparatively small, RNA specific peaks at 1120 and 995 cm^{-1}. As previously reported on single-stranded phosphodiester and phosphorothioate oligodeoxyribonucleotides, hydration alone does not induce the characteristic shift of the $\nu_{asym}(PO_2^-)$; a cooperative change in the conformation of the entire molecule must take place (35). For this reason, the RNA spectra series lacks the $\nu_{asym}(PO_2^-)$ shift. The sigmoidal shape generated in trend plots showing the position of the $\nu_{asym}(PO_2^-)$ peak versus degree of hydration is similar to that observed in a cooperative system such as oxygen binding to hemoglobin and is typical of many reversible enzymatic systems where a known quaternary structural change facilitates the rate of enzymatic activity. This is in contrast to the plot of the position of the ν(C–C) mode which is more linear with respect to hydration but still has some sigmoidal character. More work is required to interpret which bands are definitive conformation bands and which bands are more affected by direct hydration but the above results along with earlier studies by White *et al.* (35) appear to indicate that the $\nu_{asym}(PO_2^-)$ is in fact sensitive to DNA conformational change and not direct hydration.

In monitoring the subtle spectral changes of dehydrating and rehydrating samples, the primary principal component (PC1) loadings and second derivatives most clearly show peak positions associated with the B- and A-like DNA. Moreover, the loadings indicate that one of the major changes in the infrared spectrum of both dehydrating and rehydrating cells is very similar to the B to A conformational change observed in pure DNA in response to hydration, cation and ethanol concentration (36–38).

While this transition was anticipated as a reversible event in the DNA film series it was somewhat surprising that the infrared signature of this transition is replicated so closely in the spectral series of nuclei and cells during both dehydration and rehydration. DNA within cells does not exist in either a pure B- or A-form due to the bending induced by both local looping around histone octamers to form nucleosomes and the negative supercoiling caused by the negatively charged phosphate backbone (14). *In situ* DNA is also constantly dynamically interacting with proteins, neighboring nucleic acid and counter-ions during transcription, replication and in the dormant state. Nonetheless, the majority of DNA in cells has always been assumed to take on a B-like form and *in vitro* experimentation has supported this assumption (14,27). The hypothesized ability of *in situ* DNA to transition to an A-like conformation while retaining functionality has generally been restricted to short sequences of the DNA (5–9) or through saturation with DNA protecting proteins as demonstrated in some spores (11,12). Contradicting this assumption is the fact that the concordance between PC1 loadings indicates an averaged conformational shift from B- to A-like DNA during dehydration. FTIR spectroscopy cannot demonstrate a complete transformation of the *in situ* genomic DNA due to acquired spectra representing an average of all of the DNA within the cell, however the absorbance spectra, second derivative spectra, trend plots and PCA plots clearly show a general shift from majority B-like in the hydrated state to majority A-like in the dehydrated state. Similarly, those sections of DNA in an A-like conformation in the native hydrated state are not detected clearly in infrared spectra of hydrated cells because they do not constitute a large enough proportion of the DNA to influence peak position. This undoubtedly includes those stretches of DNA known to be A-philic and those interacting with proteins or ions which induce the A conformation. The presence of B-like DNA with A-like sugar conformations (39) is also undetectable, because those absorption bands influenced strongly by sugar conformation

are relatively small and located in proximity to large protein or phosphate bands.

The absorbance spectral series of dehydrating DNA, nuclei and cells show clearly that the B to A transition also results in band broadening and intensity loss in the $\nu_{sym}(PO_2^-)$ and ν(C–O) backbone absorption intensities. In the hydrated cell spectra these bands are seen as sharp, specifically located peaks. In concordance with this, both the second derivative spectra and PC1 loadings show strong shoulders at 1100 and 1063 cm^{-1} in all dehydrated samples. These changes in the DNA peaks of all samples are indicative of the transition from the native B-like DNA found in live, hydrated cells to an A-like structure in a non-homogenous environment. During dehydration the shielding of proximate cellular macromolecules is expected to be significantly diminished allowing for steric and van der Waals interactions that are far less common in the hydrated environment. These interactions cause infrared absorptions, particularly those associated with exposed parts of the DNA, namely the backbone, to broaden.

With this important aspect of the dehydrated A-like structural environment noted, it becomes even more remarkable that the DNA monitored inside dehydrated chicken erythrocyte nuclei and intact chicken erythrocytes, as well as mammalian lymphocytes and fibroblasts, can be rehydrated to the B-like DNA native to live cells. The spectra of live cells and cells rehydrated from a dehydrated state demonstrate that the transition is largely reversible with potential for only small localized conformational differences existing. This transition from B-like DNA to an A-like form under stress from proximate molecules in cells during dehydration possibly plays an important role in the ability of microorganisms such as yeast and bacteria to regain full functionality from a lyophilized state (40). The necessity of dehydrating the cell samples to an extent where a full B to A transition was confirmable and to then hold them in this dehydrated state for several hours ruled out any possibility of keeping the cells alive during the experiment. However the intact nature of the cells upon rehydration and the native-state B-like structure observed demonstrate the potential implications of this result. As such, the conservation of structural integrity of DNA via a B to A-like transition enabling a return to the native state in *in situ* cellular DNA potentially may allow elucidation of the mechanisms by which various cells have previously been shown to survive dehydration both naturally and through lyophilization methods (40,41). Furthermore, the ability of dehydrated A-like DNA to retain the ability to return to a B-like functional state is an important consideration in recent work to enable the long-term storage of somatic cells in a dehydrated state for clinical use (40,41).

A further important aspect of the band broadening and overall loss of intensity in the $\nu_{sym}(PO_2^-)$ and ν(C–O) absorptions of A-like DNA spectra is that, in this state, detection becomes inherently more difficult due to an inability to distinguish DNA specific contributions to these broad bands from the underlying peaks and shoulders due to other cellular components. The preference in the past for FTIR spectroscopy to be conducted on dehydrated biological specimens (16) has consequently encountered the problem of not detecting DNA (21). By using hydrated samples, we demonstrate the sensitivity infrared spectroscopy has, not only to the presence of DNA *in situ*, but also to conformation. As a consequence, improvements in the detection of cancer using FTIR spectroscopy are anticipated. As previously demonstrated by image cytometry, increased DNA content in dysplastic tissue as a consequence of aneuploidy results in the average amount of DNA per cell increasing from the healthy diploid value of ~6 pg to values as high as four times that (42). Neoplastic tissue will be similarly detectable due to the uncontrolled proliferation of cells resulting in a sharp decrease in the number of cells in the quiescent cell cycle phase. Instead, cells proceed from mitosis directly to interphase and consequently DNA synthesis. This result in an overall increase in the proportion of time cells contain double the amount of the genetic material and a consequent increase in the average DNA content of these neoplastic cells (43). This ability to monitor DNA concentration, along with conformation, using FTIR signifies a dramatic improvement in the examination of DNA in cells and has implications for the study of disease, cell survival in the dehydrated state, and chromatin theory.

SUPPLEMENTARY DATA

Supplementary Data are available at NAR Online.

ACKNOWLEDGEMENTS

We thank Mr Finlay Shanks (School of Chemistry, Monash) and Dr Ljiljana Puskar (Australian Synchrotron) for instrument support. The authors wish to acknowledge the Australian Synchrotron (Melbourne) for the provision of synchrotron beamtime through their merit-based access program. We acknowledge Prof. Dieter Naumann, Dr Heinz Fabian and Dr Peter Lasch (Robert Koch Institute, Germany) for helpful suggestions and verification of the main experimental results.

FUNDING

Australian Research Council Discovery Grant [DP0878464]. Funding for open access charge: Australian Research Council

Conflict of interest statement. None declared.

REFERENCES

1. Lever,E. and Sheer,D. (2010) The role of nuclear organization in cancer. *J. Pathol.*, **220**, 114–125.
2. Dickerson,R.E. (1989) Definitions and nomenclature of nucleic acid structure parameters. *J. Biomol. Struct. Dynam.*, **6**, 627–634.
3. Hunter,C.A. (1993) Sequence-dependent DNA-structure – the role of base stacking interactions. *J. Mol. Biol.*, **230**, 1025–1054.
4. Florentiev,V.L. and Ivanov,V.I. (1970) RNA polymerase - 2-step mechanism with overlapping steps. *Nature*, **228**, 519–526.

5. Eom,S.H., Wang,J.M. and Steitz,T.A. (1996) Structure of Taq polymerase with DNA at the polymerase active site. *Nature*, **382**, 278–281.
6. Tolstorukov,M.Y., Jernigan,R.L. and Zhurkin,V.B. (2004) Protein-DNA hydrophobic recognition in the minor groove is facilitated by sugar switching. *J. Mol. Biol.*, **337**, 65–76.
7. Lu,X.J., Shakked,Z. and Olson,W.K. (2000) A-form conformational motifs in ligand-bound DNA structures. *J. Mol. Biol.*, **300**, 819–840.
8. Minasov,G., Tereshko,V. and Egli,M. (1999) Atomic-resolution crystal structures of B-DNA reveal specific influences of divalent metal ions on conformation and packing. *J. Mol. Biol.*, **291**, 83–99.
9. Rich,A. (2006) Discovery of the hybrid helix and the first DNA-RNA hybridization. *J. Biol. Chem.*, **281**, 7693–7696.
10. Trantirek,L., Stefl,R., Vorlickova,M., Koca,J., Sklenar,V. and Kypr,J. (2000) An A-type double helix of DNA having B-type puckering of the deoxyribose rings. *J. Mol. Biol.*, **297**, 907–922.
11. Lee,K.S., Bumbaca,D., Kosman,J., Setlow,P. and Jedrzejas,M.J. (2008) Structure of a protein-DNA complex essential for DNA protection in spores of Bacillus species. *Proc. Natl Acad. Sci. USA*, **105**, 2806–2811.
12. Mohr,S.C., Sokolov,N., He,C.M. and Setlow,P. (1991) Binding of small acid-soluble spore proteins from *Bacillus-subtilis* changes the conformation of DNA from B to A. *Proc. Natl Acad. Sci. USA*, **88**, 77–81.
13. Dextraze,M.E., Wagner,J.R. and Hunting,D.J. (2007) 5-Bromodeoxyuridine radiosensitization: conformation-dependent DNA damage. *Biochemistry*, **46**, 9089–9097.
14. Richmond,T.J. and Davey,C.A. (2003) The structure of DNA in the nucleosome core. *Nature*, **423**, 145–150.
15. Taillandier,E. and Liquier,J. (1990) In Vasilescu,D., Jaz,J., Packer,L. and Pullman,B. (eds), *Water and Ions in Biomolecular Systems*. Birkhauser, Basel, pp. 71–78.
16. Wang,T.D., Triadafilopoulos,G., Crawford,J.M., Dixon,L.R., Bhandari,T., Sahbaie,P., Friedland,S., Soetikno,R. and Contag,C.H. (2007) Detection of endogenous biomolecules in Barrett's esophagus by Fourier transform infrared spectroscopy. *Proc. Natl Acad. Sci. USA*, **104**, 15864–15869.
17. Diem,M., Griffiths,P.R. and Chalmers,J.M. (2008) *Vibrational Spectroscopy for Medical Diagnosis*. Wiley, West Sussex, England.
18. Macallan,D.C., Fullerton,C.A., Neese,R.A., Haddock,K., Park,S.S. and Hellerstein,M.K. (1998) Measurement of cell proliferation by labeling of DNA with stable isotope-labeled glucose: Studies in vitro, in animals, and in humans. *Proc. Natl Acad. Sci. USA*, **95**, 708–713.
19. Zentgraf,H., Duemling,B. and Franke,W.W. (1969) Isolation and characterisation of nuclei from bird erythrocytes. *Exp. Cell Res.*, **56**, 333–337.
20. Tobin,M., Puskar,L., Barber,R., Harvey,E.C., Heraud,P., Wood,B.R., Bambery,K.R., Dillon,C.T. and Munroe,K.L. (2010) FTIR spectroscopy of single cells in aqueous media by synchrotron IR microscopy using microfabricated sample holders. *Vib. Spec.*, **53**, 34–38.
21. Mohlenhoff,B., Romeo,M., Diem,M. and Wood,B.R. (2005) Mie-type scattering and non-Beer-Lambert absorption behavior of human cells in infrared microspectroscopy. *Biophys. J.*, **88**, 3635–3640.
22. Clegg,J.S. (1988) L-929 cells under hyperosmotic conditions – water, Na+ and K+. *Cell Biophysics*, **13**, 119–132.
23. Wood,B.R., Tait,B. and McNaughton,D. (2000) Fourier transform infrared spectroscopy as a method for monitoring the molecular dynamics of lymphocyte activation. *Appl. Spectrosc.*, **54**, 353–359.
24. Shimanouchi,M., Tsuboi,M. and Yoshimasa,K. (1964) In Duchesne,J. (ed.), *Advance in Chemical Physics: Volume VII*, Vol. 7. John Wiley & Sons, Inc., pp. 435–498.
25. Pohle,W. and Fritzsche,H. (1980) A new conformation-specific infrared band of A-DNA in films. *Nucleic Acids Res.*, **8**, 2527–2535.
26. Liquier,J., Akhebat,A., Taillandier,E., Ceolin,F., Dinh,T.H. and Igolen,J. (1991) Characterization by FTIR spectroscopy of the oligioribonucleotide duplexes $r(A\text{-}U)_6$ and $r(A\text{-}U)_8$. *Spectrochim. Acta A Mol. Biomol. Spectrosc.*, **47**, 177–186.
27. Banyay,M., Sarkar,M. and Graslund,A. (2003) A library of IR bands of nucleic acids in solution. *Biophys. Chem.*, **104**, 477–488.
28. Hartman,K.A., Lord,R.C. and Thomas,G.J. (1973) In Duchesne,J. (ed.), *Physico-Chemical Properties of Nucleic Acids*, Vol. 2. Academic Press, New York.
29. Pevsner,A. and Diem,M. (2001) Infrared spectroscopic studies of major cellular components. Part II: the effect of hydration on the spectra of nucleic acids. *Appl. Spectrosc.*, **55**, 1502–1505.
30. Jangir,D.K., Tyagi,G., Mehrotra,R. and Kundu,S. (2010) Carboplatin interaction with calf-thymus DNA: a FTIR spectroscopic approach. *J. Mol. Struct.*, **969**, 126–129.
31. Marty,R., N'Soukpoe-Kossi,C.N., Charbonneau,D., Weinert,C.M., Kreplak,L. and Tajmir-Riahi,H.A. (2009) Structural analysis of DNA complexation with cationic lipids. *Nucleic Acids Res.*, **37**, 849–857.
32. Tajmir-Riahi,H.A., N'Soukpoe-Kossi,C.N. and Joly,D. (2009) Structural analysis of protein-DNA and protein-RNA interactions by FTIR, UV-visible and CD spectroscopic methods. *Spectrosc. Int. J.*, **23**, 81–101.
33. Tsai,A.G., Engelhart,A.E., Hatmal,M.M., Houston,S.I., Hud,N.V., Haworth,I.S. and Lieber,M.R. (2009) Conformational variants of duplex DNA correlated with cytosine-rich chromosomal fragile sites. *J. Biol. Chem.*, **284**, 7157–7164.
34. Zhang,S.L., Michaelian,K.H. and Loppnow,G.R. (1998) Vibrational spectra and experimental assingments of thymine and nine of its isotopomers. *J. Phys. Chem.*, **102**, 461–470.
35. White,A.P., Reeves,K.K., Snyder,E., Farrell,J., Powell,J.W., Mohan,V., Griffey,R.H. and Sasmor,H. (1996) Hydration of single-stranded phosphodiester and phosphorothioate oligodeoxyribonucleotides. *Nucleic Acids Res.*, **24**, 3261–3266.
36. Ivanov,V.I., Minchenkova,L.E., Minyat,E.E., Frank-Kamenetskii,M.D. and Schyolkina,A.K. (1974) B to A transition of DNA in solution. *J. Mol. Biol.*, **87**, 817–833.
37. Nejedly,K., Chladkova,J., Vorlickova,M., Hrabcova,I. and Kypr,J. (2005) Mapping the B-A conformational transition along plasmid DNA. *Nucleic Acids Res.*, **33**, e5.
38. Xu,Q.W., Shoemaker,R.K. and Braunlin,W.H. (1993) Induction of B-A transition of deoxyoligonucleotides by multivalent cations in dilute aqeous solution. *Biophys. J.*, **65**, 1039–1049.
39. Rich,A. (2003) The double helix: a tale of two puckers. *Nat. Struct. Biol.*, **10**, 247–249.
40. Loi,P., Matsukawa,K., Ptak,G., Clinton,M., Fulka,J., Nathan,Y. and Arav,A. (2008) Freeze-dried somatic cells direct embryonic development after nuclear transfer. *Plos One*, **3**, e2978.
41. Katayose,H., Matsuda,J. and Yanagimachi,R. (1992) The ability of dehydrated hamster and human sperm nuclei to develop into pronuclei. *Biol. Reproduct.*, **47**, 277–284.
42. Fang,M., Lew,E., Klein,M., Sebo,T., Su,Y.Y. and Goyal,R. (2004) DNA abnormalities as marker of risk for progression of Barrett's esophagus to adenocarcinoma: image cytometric DNA analysis in formalin-fixed tissues. *Am. J. Gastroenterol.*, **99**, 1887–1894.
43. Boydston-White,S., Gopen,T., Houser,S., Bargonetti,J. and Diem,M. (1999) Infrared spectroscopy of human tissue. V. Infrared spectroscopic studies of myeloid leukemia (ML-1) cells at different phases of the cell cycle. *Biospectroscopy*, **5**, 219–227.